Multivalent 4-1BB binding aptamers costimulate CD8+ T cells and inhibit tumor growth in mice

James O. McNamara II,[1] Despina Kolonias,[2] Fernando Pastor,[2] Robert S. Mittler,[3] Lieping Chen,[4] Paloma H. Giangrande,[1] Bruce Sullenger,[1] and Eli Gilboa[2]

[1]Department of Surgery, Duke University Medical Center, Durham, North Carolina, USA. [2]Department of Microbiology and Immunology, Dodson Interdisciplinary Immunotherapy Institute, University of Miami Miller School of Medicine, Miami, Florida, USA. [3]Department of Surgery and Emory Vaccine Center, Emory University, Atlanta, Georgia, USA. [4]Department of Dermatology, Johns Hopkins University School of Medicine, Baltimore, Maryland, USA.

4-1BB is a major costimulatory receptor that promotes the survival and expansion of activated T cells. Administration of agonistic anti–4-1BB Abs has been previously shown to enhance tumor immunity in mice. Abs are cell-based products posing significant cost, manufacturing, and regulatory challenges. Aptamers are oligonucleotide-based ligands that exhibit specificity and avidity comparable to, or exceeding, that of Abs. To date, various aptamers have been shown to inhibit the function of their cognate target. Here, we have described the development of an aptamer that binds 4-1BB expressed on the surface of activated mouse T cells and shown that multivalent configurations of the aptamer costimulated T cell activation in vitro and mediated tumor rejection in mice. Because aptamers can be chemically synthesized, manufacturing and the regulatory approval process should be substantially simpler and less costly than for Abs. Agonistic aptamers could therefore represent a superior alternative to Abs for the therapeutic manipulation of the immune system.

Introduction

In addition to antigen-dependent TCR signaling, multiple costimulatory pathways regulate the potency, duration, and type of the T cell response. Experimental manipulation of costimulatory pathways offers an attractive way to modulate immune responses for therapeutic purposes. 4-1BB is a major costimulatory receptor promoting the survival and expansion of activated T cells (1–4). It is transiently upregulated on activated T cells during primary and recall responses, and its ligand, 4-1BBL, is expressed on activated antigen-presenting cells including dendritic cells. Despite the fact that 4-1BB is upregulated on both $CD4^+$ and $CD8^+$ T cells, current evidence suggests that in vivo 4-1BB costimulates primarily $CD8^+$, and not $CD4^+$, T cells (1, 4). Because $CD8^+$ T cells play a pivotal role in tumor immunity, enhancing 4-1BB costimulation could promote the generation of protective antitumor immune responses. Consistent with this hypothesis, tumor cells engineered to express 4-1BBL (5–8) or a single-chain anti–4-1BB Ab (9) exhibited enhanced immunogenicity in mice. In addition, systemic administration of agonistic anti–4-1BB Abs enhanced tumor immunity and tumor rejection in mice (10–18).

An increasing number of clinical trials with partially or fully humanized Abs targeting CTLA-4, CD40, 4-1BB, OX-40, and PD-1 are currently underway (reviewed in refs. 19, 20). One major limitation of using monoclonal Abs as therapeutics is limited, and at best uncertain, access to this class of biologicals. A main reason is that Abs are cell-based products posing significant cost, manufacturing, and regulatory challenges. Hence clinical-grade Abs are almost exclusively developed and provided by companies on a selective basis and under strict contractual agreement. Thus, despite promising observations from murine preclinical tumor models, the use of Abs in clinical settings is restricted.

Aptamers are high-affinity single-stranded nucleic acid ligands that can be isolated from combinatorial libraries through an iterative process of in vitro selection known as systematic evolution of ligands by exponential enrichment (SELEX) (21, 22). Aptamers exhibit specificity and avidity comparable to or exceeding that of Abs and can be generated against most targets (23–25). Unlike Abs, aptamers can be synthesized in a chemical process and hence offer significant advantages in terms of reduced production cost and simpler regulatory approval processes.

In many instances aptamers have been shown to inhibit the function of their targets, presumably by blocking binding of the cognate ligand (24, 25). An aptamer targeting VEGF became the first aptamer approved for human therapy to treat age-related macular degeneration, arguably a milestone in the application of aptamer technology (26). A second aptamer targeting the coagulation factor IXa is currently being tested as an anticoagulant in phase I/II clinical trials (27). In a first demonstration of using aptamers to modulate immune responses in vivo, we previously described the generation of aptamers that bind and inhibit the function of murine CTLA-4 (28).

It has long been recognized that receptor oligomerization on the cell surface is the mechanism by which many ligands activate their cognate cell surface receptors. For example, optimal stimulation of the members of the TNF receptor family, which includes 4-1BB, involves oligomerization of individual receptors into higher-order homotrimer complexes at the immunological synapse (1). The development of artificial ligands to activate cell surface receptors via oligomerization poses significant challenges for therapeutic development. Small-molecule drugs, which are the mainstay of

Nonstandard abbreviations used: DPBS, Dulbecco PBS; SELEX, systematic evolution of ligands by exponential enrichment.

Conflict of interest: Eli Gilboa and Bruce A. Sullenger own stock in Regado Biosciences, a company developing aptamers to prevent clotting.

Citation for this article: *J. Clin. Invest.* **118**:376–386 (2008). doi:10.1172/JCI33365.

A

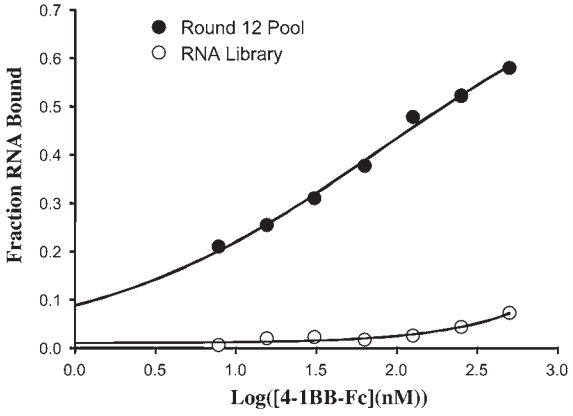

B

Random Region Sequence	# Identical Clones
GCACAGCAACACCACGAC**CCCCCCCUAGGCUUC**CGCCCGCG[#]	5*
UAACGGCCCAAUGACUUCGCCUUCUG**CCCCCCCUAAGCUUC**[#1]	1
UAACGGCCCAAUGACUUCGCCUUACUG**CCCCCCCUAAGCUUC**	1
GACCAAGGGCAGCAUCACCGUUC**CCCCCCCUAGGAGCUUAC**[#1]	1
CGAGAACCCGCAUCUUCGGAUGCG**CCCCCCCUAGGACUUAC**[#2]	1
AAGACGAUACCUAGCCUCAAAAUUCCU**CCCCCCGACUUCC**U	1
AAAGCGACAAUUCUUACUACU**CCCCAAGCUCC**ACGCCUUU	1
CGACCGAACGUGCCCUUCAAAGCCGUUCACUAACCAGUGG[#]	10*
GCACCAAAC**ACCGGUUCAGAACCCAUC**AUGUAACUCCUUG[#]	1
AACUACCUCCUCGA**ACCAUAGUUCAACACCAUC**CAGCCAU[#]	1
CGCUCUCUCACAACCACGACCUCCGAUCUGAUAAUUCGUC	2
CUCCUAGACAGACGAUGUCUGAACGACUCUUGAAGGGCAG[#2]	1
CCGCCAUUAACCCUGAACAGAAUCUUCCUAUCCCAACCCG	1
UCACCCGACGAUACCUAACUUCCUCCGACAAGCCUUUGCC	1
GCACAACAUCCUCNGUGANACCACACUUCGCCAANCUCUG[#]	1
AUCAGUACAUGCUCCGGGGCAGCCGAAUAUCUCGCGCUU[#]	1
GACCACCACAGCGACAGGCUCGCACGACUCUCGAAGAGG	1
CAAGCACUCUUCAGGCUAAGGACUCUCUUGACACCCCGC[#]	1
CCUCCUUCCUAACCCGCAAACACGAUUGGCUCGAAACUUC	1
AACCGACCGCAGAUCUGGACACUAGCUUUCGCGAGGAUU	1
GCUUCUACAGGGGGUAAAGAUUCGCUCAUCACUCGCAAAA	1

Figure 1

Isolation of aptamers that bind to murine 4-1BB. (**A**) Binding of the starting RNA library and round 12 RNA pool to 4-1BB–Fc using the filter binding assay as described in Methods. (**B**) Sequence of random regions of clones isolated from round 12 pool. Bold text denotes identical or closely related sequences. [#]Tested for binding to 4-1BB–Fc. *The final base of the random regions of these clones was variable. [1,2]Binding was measured as a mixture of each pair.

molecular medicine, are not well suited for this purpose given their small size. This is perhaps the reason why agonistic Abs, which are multivalent by nature but substantially more expensive to produce, are currently being developed for clinical use (19, 20).

Aptamers that function as agonists, such as aptamers that induce downstream signaling upon binding to cell surface receptors, have not been described so far. In this study we describe the generation of an aptamer that binds 4-1BB on the surface of activated T cells and define conditions whereby it functions as an agonist. Specifically, we showed that bivalent and multivalent configurations of the aptamers costimulated T cell activation in vitro and promoted tumor rejection in vivo. The experimental strategy described in this study should be applicable for developing agonistic aptamers targeting a broad range of cell surface–expressed mediators of stimuli such as receptors for other immune costimulatory ligands, cytokines, or growth factors. The approach described here thus provides a new set of tools to control human disease.

Results

Isolation of aptamers that bind to murine 4-1BB and costimulate CD8⁺ T cells. SELEX was used to screen a combinatorial RNA library of more than 10^{14} species for members capable of binding to the extracellular domain of murine 4-1BB. To enhance the nuclease stability of the resulting aptamers in cell culture and in vivo, the starting library and the subsequent RNA pools were generated with 2′-fluoro-pyrimidines. Progress of the selection was monitored by measuring the binding affinity of the RNA pools every other round. After 12 rounds, the RNA pool was found to have an equilibrium K_d of approximately 40 nM (Figure 1A). At this point, PCR products encoding individual aptamers were cloned and sequenced (Figure 1B). The amplification products from round 12 revealed limited sequence diversity, with unique sequences represented multiple times, indicating that the selection was nearing the end. Representative aptamers from each of the families of related sequences were tested for their ability to bind the 4-1BB extracellular domain. Several of these aptamers exhibited similar or higher affinities for 4-1BB compared with the round 12 aptamer pool (data not shown).

The ability of the 4-1BB aptamers to costimulate CD8⁺ T cells was tested in vitro by determining whether addition of aptamer will enhance the proliferation of suboptimally stimulated CD8⁺ T cells. We tested several 4-1BB binding aptamers shown in Figure 1B, yet none of them exhibited a costimulatory effect (data not shown). This was to be expected because 4-1BB, like many cell surface receptors, requires cross-linking to initiate the downstream signaling cascade (1), and the selected 4-1BB aptamers, unlike Abs, are monovalent. We therefore generated multivalent 4-1BB aptamers by transcriptionally attaching a biotin moiety to the 5′ end of the aptamer and binding the biotinylated aptamers to streptavidin-coated beads. Unlike the monovalent aptamers, a subset of the bead-attached multimeric 4-1BB aptamers exhibited a costimulatory effect (data not shown). Aptamer M12-23 exhibited the most potent costimulatory effect and was chosen for further study.

Figure 2A shows the sequence and a computer-predicted secondary structure of the M12-23 aptamer. To control for the function of M12-23, we generated an aptamer containing 5 nucleotide changes designed to disrupt the putative secondary structure (mutM12-23; Figure 2A). M12-23 bound to 4-1BB with high affinity (K_d ~40 nm), comparable to that of the round 12 aptamer pool, whereas mutM12-23 failed to bind to 4-1BB above background levels (data not shown). In the experiment shown in Figure 2B, we evaluated the costimulatory capacity of the M12-23 aptamers. Under suboptimal stimulation of CD8⁺ T cells (using low concentrations of anti-CD3 Ab), 6.61% of the cells divided, whereas in the presence of an agonistic 4-1BB Ab, 20.3% of the cells underwent division, a 3-fold enhancement of proliferation. In the presence

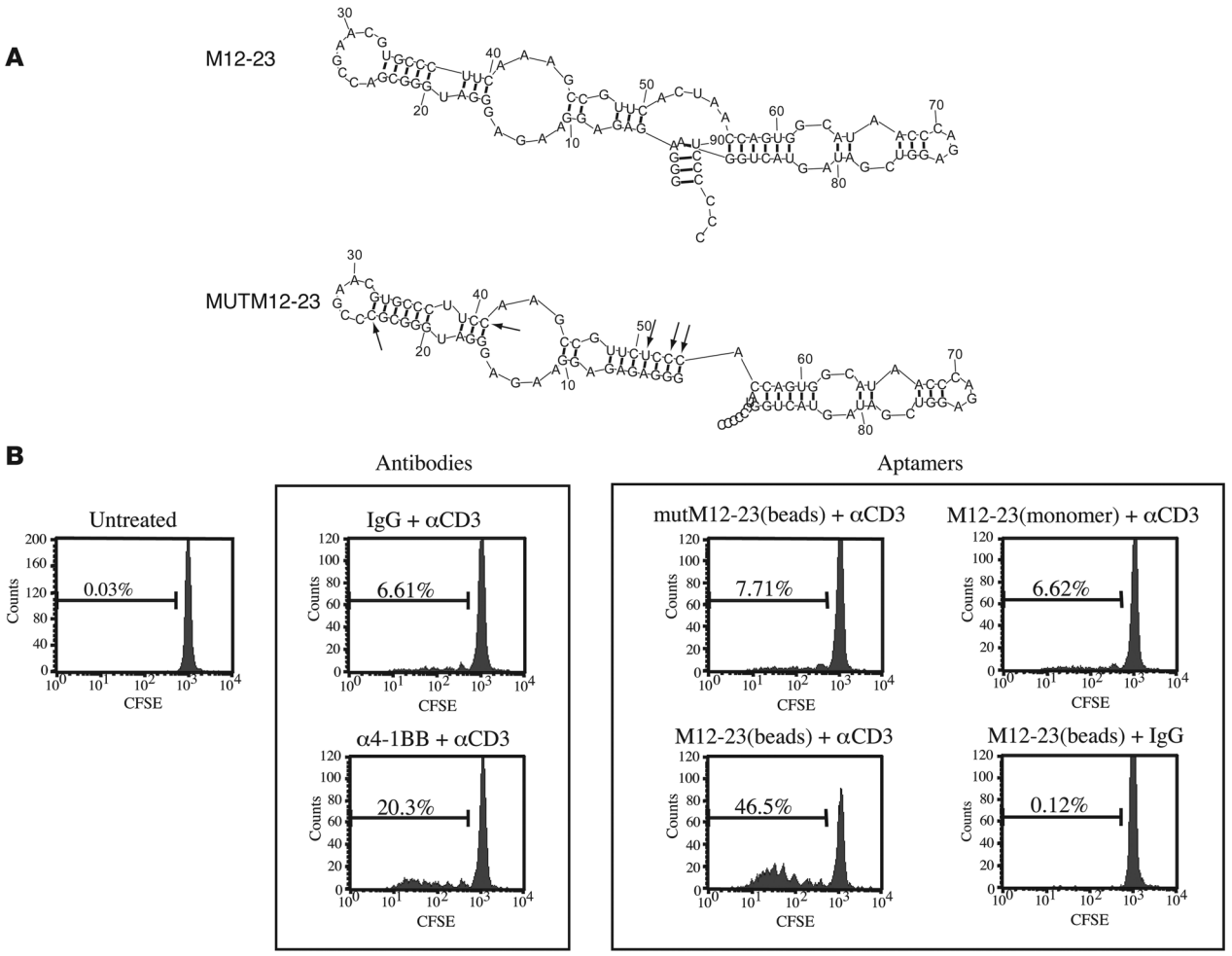

Figure 2

Characterization of M12-23 and mutM12-23 aptamers. (**A**) Sequence and computer-predicted secondary structure. Arrows show the nucleotide changes introduced into the M12-23 sequence to generate mutM12-23. (**B**) CFSE proliferation assay of suboptimally activated $CD8^+$ T cells incubated with bead-multimerized 4-1BB aptamers. $CD8^+$ T cells isolated from the spleens and lymph nodes of Balb/c mice were labeled with CFSE and cultured in the absence or presence of either 1 μg/ml anti-CD3 or isotype-matched hamster IgG control Ab. At 16 hours after plating, the following reagents were added, as indicated: 5 μg/ml anti–4-1BB Ab or isotype-matched rat IgG2a Ab, or 100 nM M12-23 aptamer (monomer), bead-coupled M12-23 aptamer, or bead-coupled mutM12-23 aptamer. Cellular fluorescence was measured with flow cytometry 72 hours after plating. Percentages within each panel indicate the fraction of cells that underwent proliferation. See Methods for additional details.

of bead-attached multivalent 4-1BB–binding M12-23 aptamers, 46.5% of T cells divided, a 7-fold enhancement of proliferation. Neither the multivalent 4-1BB–nonbinding mutM12-23 aptamer nor the monovalent 4-1BB–binding M12-23 aptamer enhanced T cell proliferation, indicating that aptamer-mediated enhanced proliferation was dependent on 4-1BB binding and cross-linking, respectively. Importantly, the proliferation seen in the presence of the bead-attached M12-23 aptamers was dependent on TCR stimulation, demonstrating that enhanced proliferation was a result of costimulation and not a direct stimulatory effect of the aptamers. These results demonstrate that an aptamer that binds to 4-1BB is capable of delivering a costimulatory signal provided it is presented in a multivalent form.

Binding of monovalent and bivalent aptamers to 4-1BB expressed on the cell surface. Administration of biotinylated aptamers attached to streptavidin-coated beads is not compatible with clinical applications. To develop a simple and clinically useful "RNA-only" approach, we generated a bivalent 4-1BB aptamer connected by a double-stranded nucleic acid linker. This was achieved by extending the 3′ end of the M12-23 aptamer with either of 2 complementary sequences and annealing the aptamers to form a dimeric structure.

The ability of the dimeric aptamers to bind and cross-link the cognate receptors is dependent on the length of the linker and the orientation or rotational freedom of the 2 monomeric aptamers. Because the 4-1BB bivalent IgG Ab is capable of inducing cross-linking of the 4-1BB receptors, we reasoned that the distance between the aptamers needs to be in the range of the distance between the 2 variable domains of the IgG Ab. Due to the flexibility of the hinge region between the Fab and Fc domains of Abs, this distance can range approximately 5–18 nanometers (29, 30). We therefore generated a 21-bp double-stranded linker providing for a 7.1-nm-long linker (3.4 nm/10 bp). The orientation of both aptamers was also controlled by the length of the linker (10 bp/helical turn), which would position the 2 aptamers in the

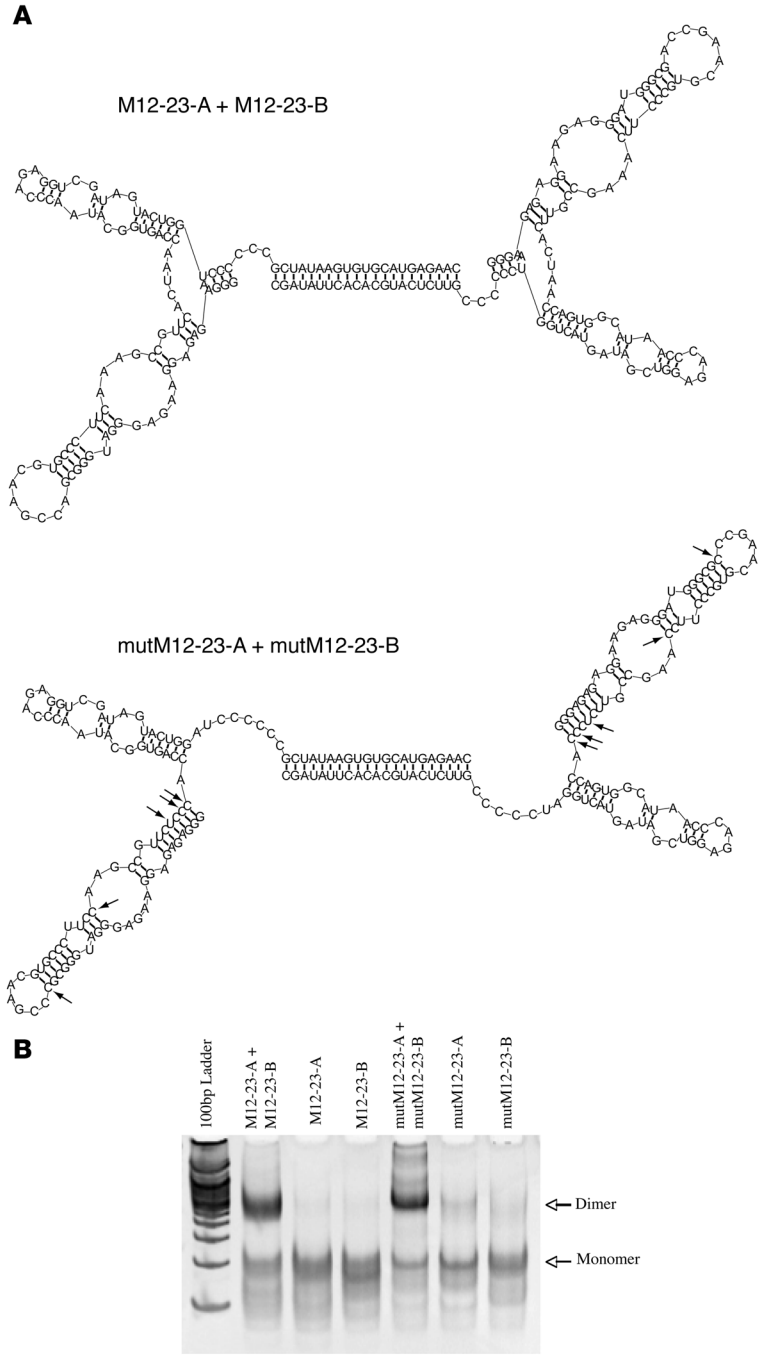

Figure 3
Structure of bivalent aptamers. Aptamer dimers were generated by adding short complementary sequences to the 3′ end of the M12-23 or mutM12-23 aptamers (denoted –A and –B) and annealing each pair. (**A**) Sequence and computer-predicted secondary structure of M12-23 and mutM12-23 dimers. Arrows show the nucleotide changes introduced into the M12-23 dimer sequence to generate mutM12-23 dimer. (**B**) Polyacrylamide gel analysis of aptamer monomers and annealing reactions. M12-23–A, M12-23–B, mutM12-23–A, or mutM12-23–B were subjected alone (2 μM each), or with 2 μM of their corresponding partners, to the annealing protocol as described in Methods. Annealing reactions were run on a nondenaturing 10% polyacrylamide gel and visualized with ethidium bromide staining.

correct orientation to interact with a pair of 4-1BB receptors. To further increase the likelihood that the dimer will bind a pair of 4-1BB receptors in the appropriate manner, we also retained the 3 nucleotide portions of the aptamers flanking the linker that were predicted to remain as single stranded. While these sequences are likely not necessary for the proper folding of the aptamers, as single-stranded sequences they may provide for rotational freedom. Dimerizing aptamers with double-stranded nucleic acids provided the means of controlling the length of the linker by increments of 0.34 nm/bp and the orientation of the aptamers (10 bp/helical turn). Thus, double-stranded nucleic acid linkers offered a framework for presenting aptamers in various configurations, increasing the likelihood that a given aptamer to a cell surface receptor can be presented in the necessary manner to stimulate its target. Figure 3A shows the sequence and computer-predicted secondary structure of the M12-23 dimer. Annealing and formation of the aptamer dimer was monitored by gel electrophoresis (Figure 3B), and the dimers were gel purified for further analysis.

The aptamers shown in Figure 1, including M12-23, were found to bind the recombinant extracellular domain of 4-1BB in a filter-binding assay. Because the agonistic effect of the natural 4-1BB ligand is mediated through binding to 4-1BB expressed on the surface of activated T cells, we determined whether the M12-23 aptamers bind 4-1BB on the cell surface. We first generated a cell line expressing 4-1BB by transfection of the human embryonic kidney cell line HEK293 with a 4-1BB expression plasmid. Expression of 4-1BB on the 4-1BB/HEK293 cells, but not the empty vector–transfected control HEK293 cells, was confirmed by flow cytometry using an anti–4-1BB Ab (Figure 4A). As shown in Figure 4A, the 4-1BB M12-23 dimer bound to 4-1BB/HEK293 but not to control HEK293 cells, whereas the control mutM12-23 aptamer dimer failed to bind to either 4-1BB/HEK293 or HEK293 cells. Figure 4B shows that at high concentration, both monomer and dimer bound to 4-1BB/HEK293 cells with equal efficiency. However, at lower concentrations, binding of the monomer was less efficient than the dimer, indicating that the avidity of the bivalent aptamer was higher than that of the monovalent aptamer. Figure 4C shows that the anti–4-1BB Ab and the M12-23 dimer, but not the control mutM12-23 aptamer, bound to activated $CD8^+$ T cells, whereas neither Ab nor aptamer bound to unstimulated T cells. Importantly, binding of the M12-23 aptamer dimer was competed by the 4-1BB Ab. These findings demonstrate that the M12-23 aptamer binds specifically to 4-1BB expressed on the surface of activated $CD8^+$ T cells.

Costimulation of $CD8^+$ T cells and inhibition of tumor growth with bivalent 4-1BB aptamers. In order to determine whether binding of the M12-23 dimers to 4-1BB delivers a costimulatory signal, we measured the proliferative capacity and secretion of IFN-γ by the suboptimally stimulated $CD8^+$ T cells. Figure 5A shows the effect of M12-23 dimers on pro-

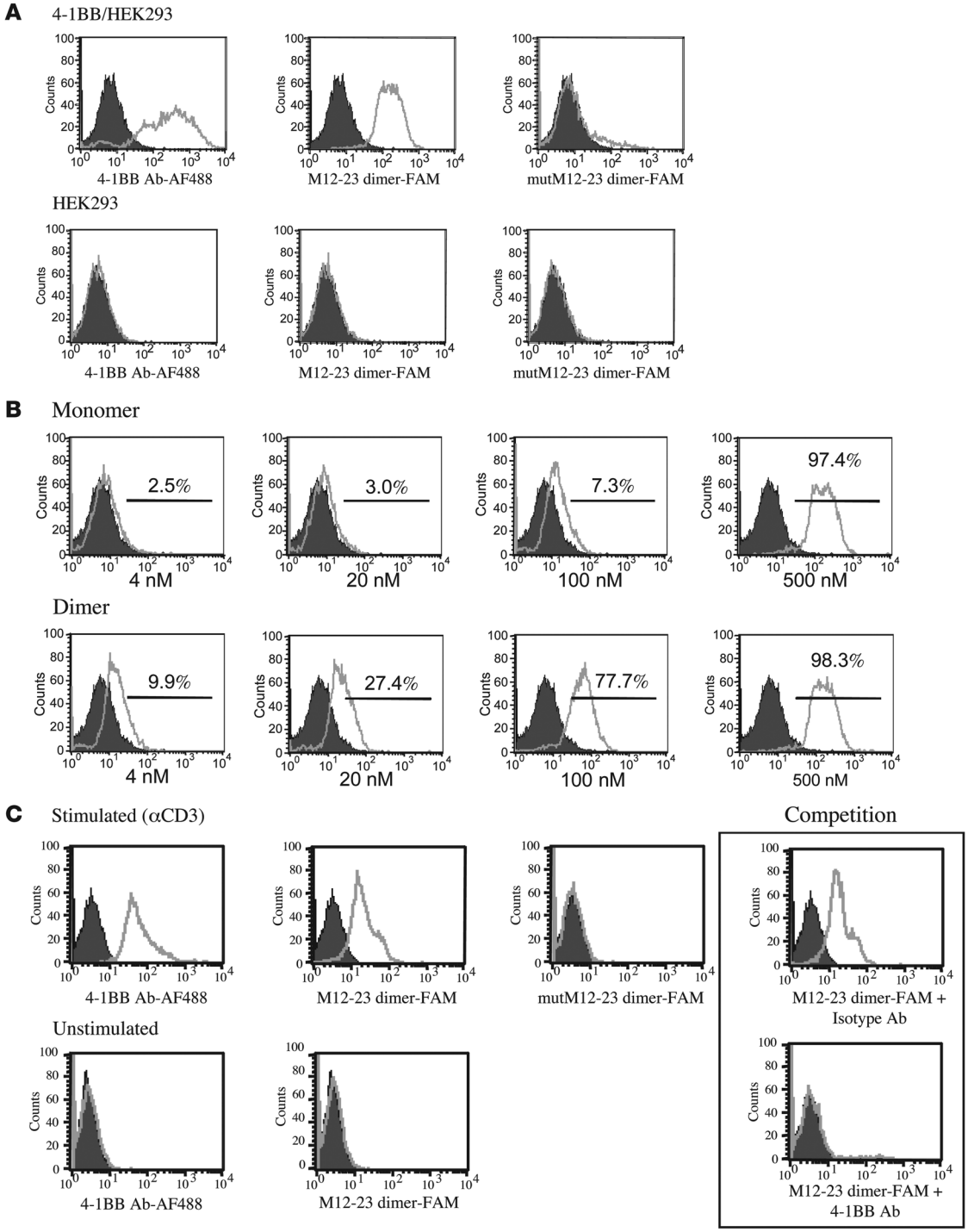

Figure 4
Binding of M12-23 aptamers to 4-1BB expressed on the cell surface. Formaldehyde-fixed cells were incubated with a 4-1BB Ab or an isotype-matched control Ab and an AF488-conjugated anti-rat IgG secondary Ab, or with FAM-labeled aptamers, and analyzed by flow cytometry. (**A**) Binding of 4-1BB Ab and M12-23 aptamer dimers to 4-1BB–transfected HEK293 cells (top panels) or empty vector–transfected control HEK293 cells (bottom panels). Background fluorescence of the 4-1BB–expressing and control HEK293 cells (shown in black) was assessed independently with a rat IgG2a primary Ab and an AF488 anti-rat IgG secondary Ab. (**B**) 4-1BB–transfected HEK293 cells were incubated with increasing concentrations of M12-23 monomers (top panels) and M12-23 dimers (bottom panels). Percentages within each panel indicate the fraction of cells that underwent proliferation. (**C**) Binding of 4-1BB Ab and M12-23 dimers to anti-CD3 Ab–stimulated and unstimulated $CD8^+$ T cells. Background fluorescence of the stimulated and unstimulated cells (shown in black) was assessed independently with a rat IgG2a primary Ab and an AF488 anti-rat IgG secondary Ab. Also, anti-CD3 Ab–stimulated $CD8^+$ T cells were preincubated with an isotype-matched control Ab or 4-1BB Ab and then incubated with FAM-conjugated M12-23 aptamer dimers; binding of the M12-23 aptamer dimer was competed by the 4-1BB Ab.

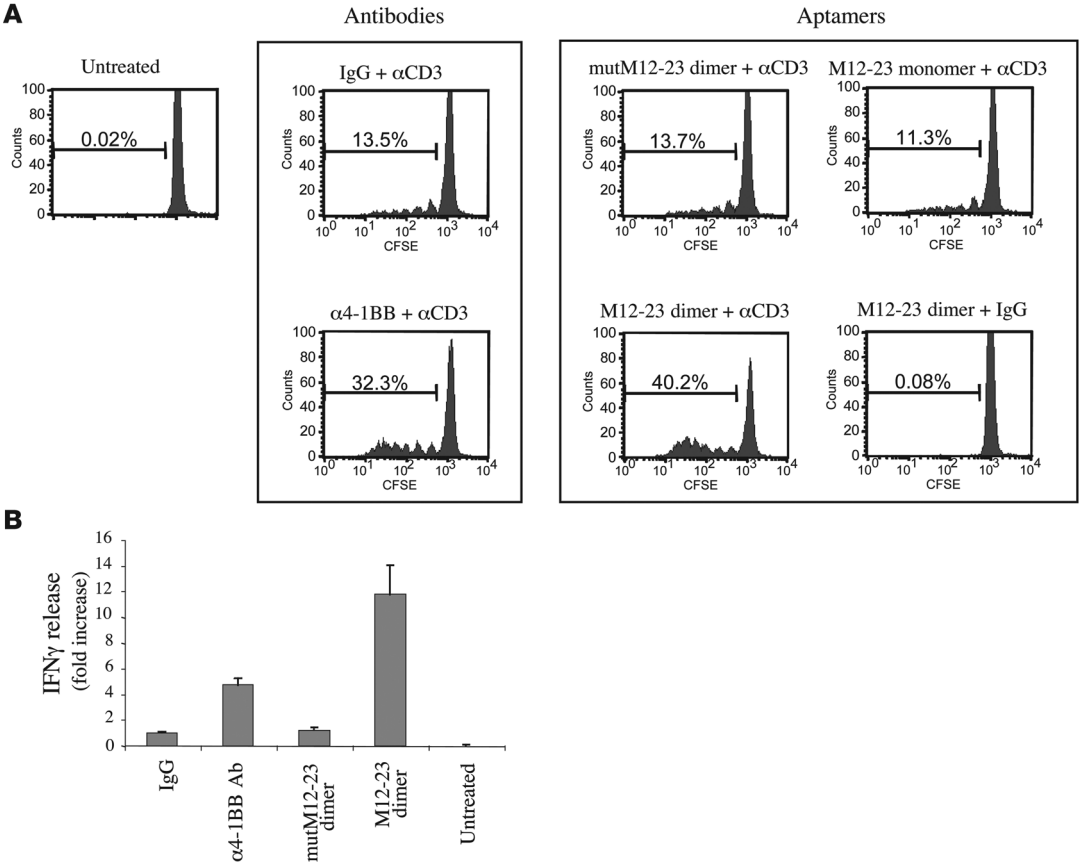

Figure 5

4-1BB costimulation with bivalent aptamers. (**A**) CFSE proliferation assay was performed essentially as described in Figure 2B except that aptamer dimers were used instead of bead-conjugated aptamers. Percentages within each panel indicate the fraction of cells that underwent proliferation. (**B**) IFN-γ secretion. $CD8^+$ T cells were stimulated with anti-CD3 Ab for 16 hours. Abs or aptamers were added as indicated and cultured for an additional 56 hours. IFN-γ in the supernatant was determined by ELISA.

liferation. The experimental design was identical to that in Figure 2B except for the use of dimers instead of bead-multimerized aptamers. In this experiment, 13%–14% of cells proliferated in response to stimulation with suboptimal concentrations of anti-CD3 Ab. Both the agonistic 4-1BB Ab and the M12-23 dimer costimulated T cell activation, as reflected in a 2.4- and 2.9-fold increase in proliferation, respectively. As seen in the experiment using bead-multimerized aptamers (Figure 2B), neither the mutant aptamer mutM12-23, which did not bind to 4-1BB on the cell surface (Figure 4), nor the monomer, which at the concentration used in this experiment bound to 4-1BB expressed on HEK293 cells (Figure 4B), exhibited costimulatory activity, and no proliferation was seen in the absence of TCR stimulation (Figure 5A). A second means of assessing the costimulatory capacity of the 4-1BB–binding aptamers is to measure the secretion of IFN-γ from the suboptimally activated $CD8^+$ T cells. As shown in Figure 5B, incubation with the 4-1BB Ab or the M12-23 aptamer dimer resulted in a 5.4- and 11.8-fold increase in IFN-γ secretion, respectively. Our results therefore show that the 4-1BB aptamer dimer is capable of costimulating T cell activation in vitro with an efficiency comparable to that of the 4-1BB Ab.

It was previously shown that administration of agonistic 4-1BB Abs can induce the regression of P815 mastocytoma tumors (10–18). To determine whether the 4-1BB aptamers are also capable of inhibiting tumor growth, P815 tumor cells were implanted subcutaneously into DBA-2 mice; when the tumors became palpable (reaching 4–5 mm in diameter), 4-1BB Ab or M12-23 4-1BB aptamer dimers were injected intratumorally. Figure 6, A–C, shows that injection of either 4-1BB Ab or 4-1BB aptamer dimer inhibited tumor growth, resulting in the regression of most tumors. Conversely, neither injection of isotype Ab nor injection of the inactive mutM12-23 aptamer dimer had an effect on tumor growth. Consistent with the differential binding (Figure 4) and costimulating (Figure 5) properties of M12-23 and mutM12-23 aptamer dimers, the fact that the closely related mutM12-23 aptamer did not affect tumor growth argues that the tumor-inhibitory effect of the M12-23 aptamer dimers was a result of 4-1BB costimulation and not of nonspecific immune activation. Rejection of the Ab- or aptamer-injected tumors was immune mediated, as shown by the fact that the surviving mice resisted a tumor challenge 2 months after the initial tumor implantation (Figure 6D).

Discussion

Oligonucleotide-based aptamers have previously been shown to inhibit their cognate target, presumably by blocking binding of the natural ligand (25). In this study we describe an aptamer that bound to murine 4-1BB on the cell surface (Figure 4) and functioned in an agonistic manner: namely, it costimulated T cell

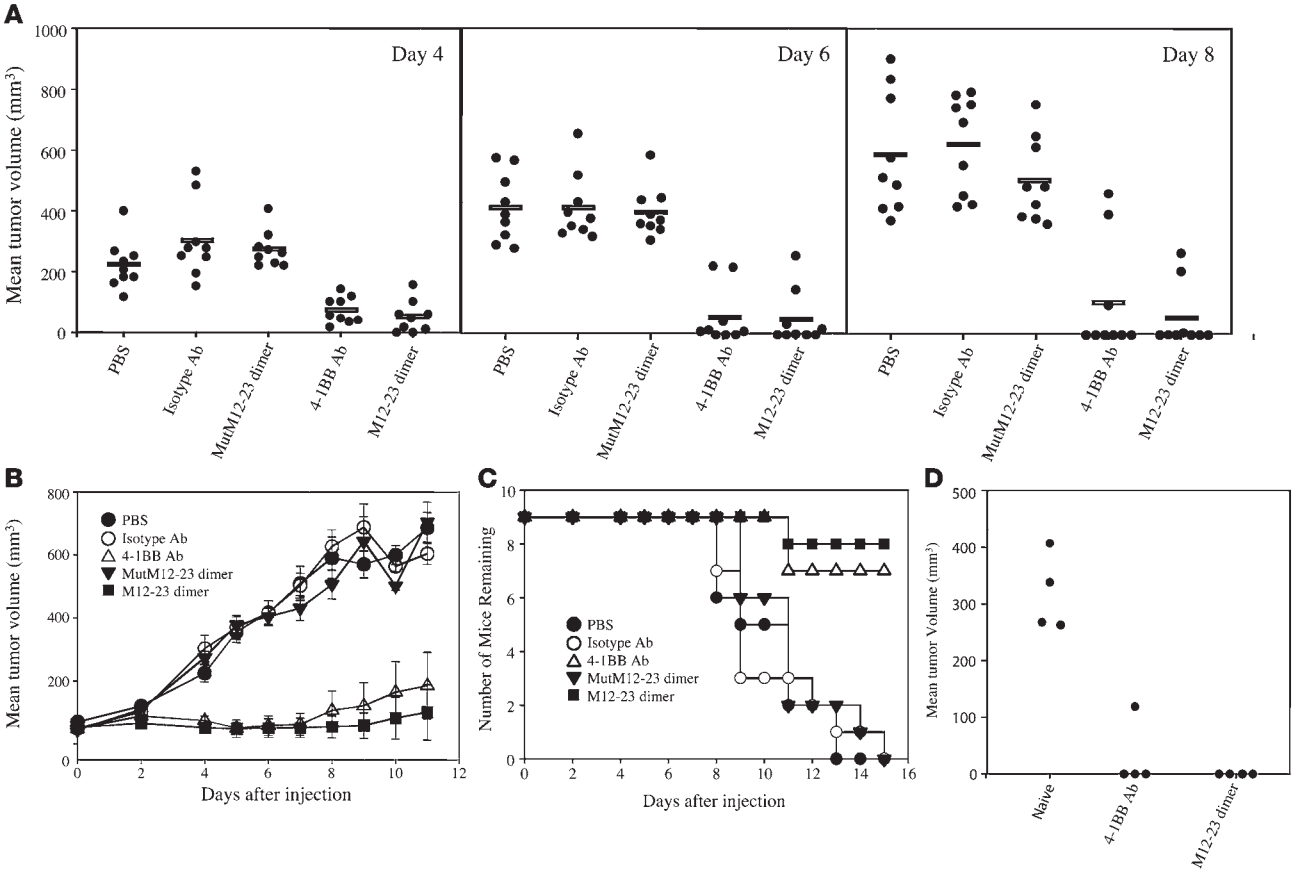

Figure 6

Regression of P815 mastocytoma tumors injected with bivalent 4-1BB aptamers. DBA-2 mice were implanted subcutaneously with 8×10^4 P815 tumor cells. When tumors became palpable, reaching an approximate diameter of 5 mm, tumors were injected with 30 μg Ab or aptamer dimer as indicated ($n = 9$ per group). Ab and aptamer dimer injections were repeated 2 days later. When tumor diameters reached or exceeded 12 mm, mice were sacrificed. (**A**) Individual tumor volumes measured 4, 6, and 8 days after injection of Ab or aptamer. Horizontal lines indicate mean tumor volumes. Differences between the control (PBS, isotype Ab, and mutM12-23 dimer) and experimental groups (4-1BB Ab and M12-23 dimer) at days 6 and 8 after injection were significant ($P < 0.001$, Student's t test). The 4-1BB Ab– and M12-23 dimer–treated groups were not significantly different. (**B**) Tumor volume. Data are mean ± SEM. (**C**) Mice without tumors or with tumors that had not reached 12 mm diameter. Differences between the control and treatment groups were statistically significant ($P < 0.01$). (**D**) Mice that rejected the implanted tumors and age-matched control mice were rechallenged with P815 tumor cells 58 days after initial tumor implantation. Individual tumor volumes 13 days after rechallenge are shown. $P < 0.01$, naive versus 4-1BB Ab. $P < 0.001$, naive versus M12-23 dimer.

activation (Figure 2B and Figure 5). In accordance with cross-linking being a requisite for signal transduction, multivalent, but not monovalent, forms of the 4-1BB aptamer were costimulation competent (Figure 2B and Figure 5). Furthermore, intratumoral injection of bivalent 4-1BB–binding aptamers induced the regression of subcutaneously implanted tumors (Figure 6). Using a similar strategy, we have isolated aptamers that bind to murine OX40 but do not costimulate T cell activation unless dimerized using complementary oligonucleotide linkers as described in this study (C.M. Dollins et al., unpublished observations).

RNA can trigger the innate immune response through families of cell surface and intracellular pathogen sensing receptors (31, 32). In addition, double-stranded RNA can activate the 2-5′ oligoadenylate synthetase/RnaseL and the PKR pathways leading to IFN-β production (33). Nonspecific immune-stimulatory effects of antisense RNA and siRNA have been noted in vitro as well as in vivo (34, 35). Our present data suggest that the costimulatory effects of the 4-1BB aptamers are not mediated by nonspecific off-target effects. First, a control aptamer with 5 point mutations in the sequence of the 4-1BB aptamer that did not bind to 4-1BB (Figure 4, A and C) failed to costimulate T cell activation (Figure 2B and Figure 5A) or induce tumor regression (Figure 6). Second, under conditions in which both monovalent and bivalent forms of 4-1BB aptamers bound to 4-1BB on the cell surface (Figure 4B), only the bivalent form exhibited a costimulatory effect (Figure 5A). Third, aptamer-mediated proliferation of T cells was dependent on TCR stimulation (Figure 2B and Figure 5).

The present study provides an initial demonstration that aptamers with agonistic functions can be generated. The potency of aptamer-based agonistic ligands is suggested by the observations that the 4-1BB–binding M12-23 dimerized aptamer, a first-generation agonistic aptamer, was comparable to a previously described anti–4-1BB Ab in binding to 4-1BB expressed on activated T cells (Figure 4C), costimulating $CD8^+$ T cells in vitro (Figure 5), and inducing tumor regression in mice (Figure 6). It is highly likely that second-generation, increasingly potent, aptamer formula-

tions can be generated. Optimal stimulation by the members of the TNF receptor family involves oligomerization of individual receptors into higher-order homotrimer complexes at the immunological synapse (1), consistent with observations that oligomeric ligands composed of 2–4 trimer repeats deliver a superior activation stimulus (36, 37). It is therefore conceivable that the costimulation potency of 4-1BB aptamers can be further improved by designing such higher order trimeric formulations.

The experiment described in Figure 6 showed that 4-1BB aptamers can mediate tumor rejection in vivo. Intratumoral injection of immune-modulatory reagents will have important but limited clinical applications. Systemic administration of immune modulators to enhance vaccine-induced immunity will have broader applications especially for targeting metastatic disease. Thus, in order to evaluate the potential of using 4-1BB aptamer to modulate systemic immunity, the pharmacological properties of the aptamers, namely their in vivo stability and bioavailability, need to be optimized. For example, the stability of aptamers in the circulation can be further enhanced by post-synthetic modifications involving substitution of the nucleoside backbone (38, 39), and the half-life of aptamers can be prolonged by conjugation to carriers such as cholesterol or polyethylene glycol (40, 41).

Aptamers correspond to a new class of therapeutic agents that offer important advantages over Abs to manipulate the immune system for therapeutic purposes. Abs are cell-based products requiring a complex and costly manufacturing and regulatory approval process that severely limits their availability for clinical exploration. Importantly, murine studies have shown that 2 or more Abs targeting complementary pathways can exert synergistic or additive effects in promoting protective antitumor immunity. For example, treatment with anti–4-1BB Ab and anti-B7H1 Ab (15) or a combination of anti–death receptor–5 (anti-DR5), anti–4-1BB, and anti-CD40 Abs (42) exhibited remarkable antitumor effects. Yet the complexity of generating and access to multiple clinical-grade Abs, often manufactured by different companies, essentially precludes their combined exploration in clinical trials. Because aptamers can be chemically synthesized, the manufacturing and regulatory approval processes should be much simpler and less costly. Additional features and advantages of aptamers compared with Abs, including reduced immunogenicity, are discussed and summarized by Nimjee and colleagues (25).

While no overt toxicities were reported in the murine tumor immunotherapy studies (10–18), closer examination has revealed that mice injected with anti–4-1BB Abs exhibited immune anomalies of transient nature mediated by polyclonal activation of $CD8^+$ T cells that were resolved upon cessation of Ab administration (43). Systemic administration of agonistic 4-1BB Abs also carries the risk of inducing or exacerbating autoimmune disease. Surprisingly, administration of agonistic 4-1BB Abs was often associated with reduced pathology in several murine autoimmune disease models (44–47). The reasons are not clear but could represent a different, apparently proapoptotic, impact of 4-1BB signaling in $CD4^+$ T cells, and secondarily humoral responses, or the induction of suppressor $CD8^+$ T cells (48). Therefore, 4-1BB therapy could provide the unexpected bonus of enhancing tumor immunity and suppressing autoimmunity. This was indeed demonstrated in a recent study showing that coadministration of blocking anti–CTLA-4 Ab together with an agonistic anti–4-1BB Ab not only enhanced antitumor immunity but also attenuated CTLA-4 Ab–induced autoimmunity (16). As discussed above, using a combination of 4-1BB and CTLA-4 aptamers may be clinically more feasible.

Methods

Selection of 4-1BB–binding aptamers. A SELEX procedure as described by Fitzwater and Polisky (49) with small modifications was used to isolate aptamers that bind a recombinant mouse 4-1BB extracellular domain/human IgG Fc fusion protein (R&D Systems). The RNA library consisted of the sequence 5′-GGGAGAGAGGAAGAGGGAUGGG-N40-CAUAACCCAGAGGUCGAUAGUACUGGAUCCCCCC-3′, where N40 represents a random sequence of 40 bases. We substituted 2′-fluoro-CTP and 2′-fluoro-UTP (Trilink) for their natural counterparts in the transcription reactions used to generate the library and subsequent rounds of RNA, yielding RNAs that were resistant to extracellular RNAses. Transcriptions were carried out with a mutant T7 RNA polymerase (Y639F; expression plasmid was a kind gift from W. McAllister, University of Medicine and Dentistry of New Jersey, Stratford, New Jersey, USA) to more efficiently incorporate these modified bases (50).

In the first round, 3.5 nmol RNA was incubated with 2.5 μM 4-1BB–Fc in 300 μl low-salt binding buffer (20 mM HEPES, pH 7.4; 50 mM NaCl; 2 mM $CaCl_2$; 0.01% BSA) at 37°C for 15 minutes. We then purified 4-1BB–binding RNA species by filtration through a nitrocellulose disc and recovered them via phenol-chloroform-isoamyl alcohol extraction. Reverse transcription, PCR, and transcription were carried out as described previously (49). Prior to incubation with 4-1BB–Fc, the library RNA was incubated with 1 μM human IgG1 (Sigma-Aldrich), also in low-salt binding buffer, and then spun through a Centrex nitrocellulose filter (Whatman) to remove sequences that would bind the Fc portion of the fusion protein. In subsequent rounds, RNA pools underwent a modified preclearing protocol to remove nonspecific sequences prior to addition of 4-1BB–Fc. Briefly, the RNA pool was incubated with human IgG1-bound Protein A Sepharose beads (10 μl beads slurry; Amersham Biosciences) in the low-salt binding buffer (rounds 2–12) at room temperature for 30 minutes on a rotator. To remove any RNA bound to Abs that may have detached from the preclearing beads, the supernatant from the first preclearing step was incubated with a prewet nitrocellulose disk (Schleicher and Schuell) at room temperature for 30 minutes on a rotator (rounds 6–12).

The precleared RNA pools were then incubated with 4-1BB–Fc–bound Protein A Sepharose beads (10 μl beads slurry; rounds 2–12) at 37°C for 30 minutes with occasional agitation. The beads were then washed with binding buffer, and the RNA was recovered with phenol-chloroform-isoamyl alcohol extraction. Because the randomized library of RNA bound 4-1BB only weakly, the initial NaCl concentration in the binding buffer was fixed at only 50 mM to increase the likelihood of recovering sequences that bind 4-1BB with high affinity but were initially present in low abundance. This concentration was increased throughout the selection until it reached 150 mM at round 9. The affinity of the pools of RNAs for recombinant 4-1BB–Fc was measured with a double-filter nitrocellulose filter binding assay (51) as modified by Layzer and Sullenger (52).

RT-PCR products from round 12 were cloned into pcDNA3.1 (Invitrogen) via EcoR1 and BamH1 restriction enzyme digestion and sequenced. The mutM12-23 sequence was generated with standard molecular biology techniques and incorporated into the pGem-t-easy vector (Promega). Aptamer transcription templates were produced by using the appropriate plasmid clones as templates in PCRs. RNA secondary structure predictions were generated with RNA Structure version 4.1 (http://rna.urmc.rochester.edu/rnastructure.html; ref. 53)

Purification of T cells. Cell culture reagents were obtained from Invitrogen unless noted otherwise. $CD8^+$ T cells were purified from the spleens and lymph nodes of BALB/c mice with a StemSep Negative selection kit (Stem Cell Technologies). After lysing the red blood cells in NH_4Cl and removing adherent cells, the procedure outlined in the manufacturer's instructions was followed closely. At the completion of the purification, cells were pelleted by centrifugation, resuspended in Dulbecco PBS (DPBS; without Ca^{2+}

and Mg^{2+}) plus 5% FBS and counted. These preparations were occasionally assayed for purity with an anti-CD8 Ab and flow cytometry and consistently found to include greater than 95% $CD8^+$ cells.

CFSE labeling and cell culture. Purified $CD8^+$ mouse T cells were labeled with 2 μM CFSE (Invitrogen) for 5 minutes at room temperature in DPBS (without Ca^{2+} and Mg^{2+}) plus 5% FBS with a cellular concentration of 10^6 cells/ml. Cells were then washed twice with DPBS (without Ca^{2+} and Mg^{2+}) plus 2% FBS and then once with complete T cell culture media (see below). Purified, CFSE-labeled or unlabeled cells were plated at 10^6 cells/well, 200 μl/well in 96-well round-bottomed culture dishes in complete T cell media (RPMI 1640 supplemented with 10% FBS, 1 mM sodium pyruvate, essential and nonessential amino acids, 100 U/ml penicillin, 100 μg/ml streptomycin, 55 μM β-mercaptoethanol, and 20 mM HEPES). Immediately after plating, anti-mouse CD3e or an isotype-matched control hamster IgG was added to the appropriate wells at 1 μg/ml. At 16 hours after plating, an anti–4-1BB Ab (5 μg/ml), an isotype-matched control Ab (rat IgG2a; 5 μg/ml), or aptamers in solution (100 nM) or coupled to beads were added to the cells.

Coupling of aptamers to streptavidin beads. Biotin was incorporated into the 5′ ends of aptamers by spiking the aptamer transcriptions with 4 mM 5′-biotin-spacer9-G (a 4-fold excess over the GTP concentration; Trilink). After gel purification, the biotinylated aptamers were diluted to 0.2 μM in binding buffer (20 mM HEPES, pH 7.4; 150 mM NaCl; 2 mM $CaCl_2$; 0.01% BSA), denatured at 65°C for 5 minutes, and allowed to fold at 37°C for 5 minutes. For each well of cells to be incubated with aptamer-coupled beads, 1.2×10^6 streptavidin magnetic beads (Dynabeads M-280 Streptavidin; Invitrogen) were washed with binding buffer and resuspended in 100 μl 0.2 μM (20 pmol) biotinylated aptamer. The bead-aptamer mixtures were incubated at room temperature for 30 minutes with occasional agitation. Beads were then washed with binding buffer, resuspended in the supernatant of a T cell culture, and added back to the culture. Upon addition of the beads to the cultures, the cells were gently dispersed from the bottom of the wells via pipetting to ensure mixing of the beads with the cells.

IFN-γ ELISA. Mouse $CD8^+$ T cells were purified, cultured, and stimulated as described above. At 72 hours after plating, the supernatants were removed and assayed with a mouse Interferon Gamma ELISA Development System kit (R&D Systems). Three wells of cells were assayed for each condition.

4-1BB aptamer dimerization. The DNA templates for the transcriptions of the dimer subunits were generated with PCR using the library 5′ oligo and either of 2 3′ oligos: M12-23–A oligo (5′-**GTTCTCATGCACACTTATAGC**-GGGGGGATCCAGTACT) or M12-23–B oligo (5′-**GCTATAAGTGTGCATGAGAAC**GGGGGGATCCAGTACT); bold sequences denote the portions that encode the dimerizing linkers. Templates for the PCRs were plasmid clones of either the M12-23 or mutM12-23 sequences. After dimer subunits were transcribed and gel purified, each pair of subunits was combined at a concentration of 2 μM each in binding buffer, denatured at 65°C for 7 minutes, and allowed to anneal at 37°C for 10 minutes. The volume was reduced by centrifugal filtration (Centricon YM-30; Millipore), and the annealed RNAs were then run on 1× Tris borate-EDTA acrylamide (nondenaturing) gels. The upper bands were excised, and the dimers were recovered by elution in Tris-EDTA at 37°C. Dimers were concentrated and washed with Tris-EDTA and then DPBS via centrifugal filtration as described above.

Generation of stably transfected HEK cells. A plasmid encoding the mouse 4-1BB extracellular domain fused to the human 4-1BB transmembrane and cytosolic domains was constructed with standard molecular biological methods. Briefly, plasmids encoding the extracellular domain of mouse 4-1BB (NIH Mammalian Gene Collection clone 41133; Invitrogen) and the full length human 4-1BB sequence (NIH Mammalian Gene Collection clone 2172; ATCC) were used as templates for PCRs, the products of which were combined to create the full-length construct. The encoded amino acid sequence of the border between the mouse and human sequences was **PEGGPGGHSL***NFFLALT*, where the sequence in bold is derived from the mouse ortholog and that in italics from the human ortholog. DNA encoding the final 5 amino acids of the mouse sequence was engineered via PCR primers because this sequence was not part of the mouse 4-1BB plasmid template.

DNA encoding this fusion protein was incorporated into the pcDNA3.1 expression vector (Invitrogen). HEK cells were transfected with the expression construct or the empty vector, and stable transfectants were selected with 600 μg/ml G418 (Invitrogen) in DMEM plus 5% FBS. Stably transfected cells expressing high levels of the mouse 4-1BB extracellular domain on their surface were isolated with fluorescence-activated cell sorting (FACS) after the cells were labeled with an anti-mouse 4-1BB Ab and an AF488-labeled anti-rat IgG.

Cell surface labeling. FAM was incorporated into the 5′ ends of aptamers by spiking the aptamer transcriptions with 4 mM 5′-FAM-spacer9-G (a 4-fold excess over the GTP concentration; Trilink). To label aptamer dimers with FAM, only 1 of the 2 monomers that made up the dimer was labeled with FAM. All other aspects of dimer generation were the same as for the unlabeled dimers.

For HEK293 cell surface labeling, cells overexpressing the mouse 4-1BB extracellular domain or cells transfected with the empty vector (pcDNA3.1$^+$) were trypsinized, washed, and fixed in DPBS plus 1% formaldehyde at room temperature for 20 minutes. Cells were then washed again with DPBS and binding buffer and then resuspended in binding buffer (200,000 cells in 100 μl per sample). Cells were warmed to 37°C, Abs (20 ng/μl) or aptamers (500 nM except where otherwise indicated) were added, and samples were incubated at 37°C for 1 hour. Cells were then washed with binding buffer. Secondary Ab (5 ng/μl) was added to appropriate samples (in binding buffer), which were then incubated at 37°C for 30 minutes. These cells were washed again with binding buffer. At the completion of the labeling and washing steps, all cells were resuspended in DPBS plus 1% formaldehyde prior to flow cytometry.

For the T cell surface labeling experiments, mouse $CD8^+$ T cells were purified and cultured as described above. Cells were used 19 hours after plating and addition of either 1 μg/ml anti-CD3e or a hamster IgG (isotype-matched control Ab). Labeling was carried out as described for HEK293 cells with the following exceptions. For each sample, 750,000 T cells were used. Following fixation, the T cells were precleared by incubation in binding buffer plus 10 ng/μl poly(I:C) (Sigma-Aldrich) at 37°C for 30 minutes. All subsequent steps were carried out in this preclearing solution. Aptamer dimer concentration was 1 μM for labeling. The preincubations of cells with Abs (20 ng/μl) was carried out at 37°C for 30 minutes in binding buffer. These samples were then washed prior to incubation with the labeled aptamers. After completion of labeling steps, cells were washed and cellular fluorescence was immediately measured with flow cytometry.

Flow cytometry. For the CFSE proliferation assays, cells were resuspended in their supernatants and then transferred to tubes containing ice cold DPBS (without Ca^{2+} and Mg^{2+}) plus 2% FBS. At this point, cells that were incubated with magnetic beads were separated from the beads via a magnetic field. Samples were then kept on ice until cellular fluorescence was measured with flow cytometry. All flow cytometry data were collected with a BD FACSCalibur flow cytometer.

Tumor implantation and monitoring tumor growth. P815 mastocytoma cells (ATCC) were grown in DMEM supplemented with 10% FBS for 2 days. Cells were washed once with DPBS and resuspended in DPBS at a concentration of 8×10^5 cells/ml. We injected 100 μl (8×10^4 cells) subcutaneously into the flanks of adult female DBA/2 mice (Jackson Laboratories). Mice were monitored every 48 hours for tumor growth. The length and width of visible tumors were measured and recorded, and intratumoral injections were begun when the longer of these measurements averaged approximately 5 mm. We injected 30 μg of 4-1BB Ab, isotype-matched

IgG2a, M12-23 aptamer dimer, or mutM12-23 aptamer dimer in 100 μl of DPBS intratumorally with a 28-gauge needle. Injections were repeated once 48 hours after the first injection for a total of 2 injections per tumor. Tumors were measured prior to each injection, 2 days after the second injection, and then every 24 hours until the termination of the experiment. Animals were sacrificed when either the length or the width of their tumors exceeded 12 mm. Tumor volumes were approximated based on the assumption that the tumor was spherical in shape. For the purpose of calculating tumor volumes, the mean of the tumor length and width was taken as the diameter. The Institutional Animal Care and Use Committee of Duke University approved the procedures involved in the harvest of tissues for the in vitro assays. Animal care and use have been approved by the University of Miami Institutional Animal Care and Use Committee Office as stipulated by the US Government in Principles of Utlization and Care of Vertebrate Animals Used: Testing, Research, and Training.

Abs for functional assays, cell surface labeling, and animal experiments. Anti-mouse CD3e, isotype-matched control hamster IgG, and control rat IgG2a were all obtained from eBioscience. The rat anti-mouse 4-1BB Ab (clone 3H3) was previously described (54). The AF488 anti-rat IgG was obtained from Invitrogen.

Statistics. Student's *t* tests were preformed to determine statistical significance of differences between tumor sizes in the experimental and control groups for both the initial tumor immunotherapy and the tumor challenge experiments. *P* values less than 0.05 were considered significant.

Acknowledgments

This work was supported in part by grant 1R01 CA 104356 from the NIH and the National Cancer Institute. J.O. McNamara II was a recipient of an NIH training grant (5T32CA00911-28). We wish to thank Kyung Hee Yi for assistance with the mouse studies.

Received for publication July 23, 2007, and accepted in revised form October 29, 2007.

Address correspondence to: Eli Gilboa, Department of Microbiology and Immunology, Sylvester Comprehensive Cancer Center, University of Miami Miller School of Medicine, 1550 NW 10th Avenue Medical Campus, PO Box 019132 (M877), Miami, Florida 33101, USA. Phone: (305) 243-1767; Fax: (305) 243-4409; E-mail: egilboa@med.miami.edu.

James O. McNamara II and Paloma H. Giangrande's present address is: Department of Internal Medicine, University of Iowa Carver College of Medicine, Iowa City, Iowa, USA.

1. Croft, M. 2003. Co-stimulatory members of the TNFR family: keys to effective T-cell immunity? *Nat. Rev. Immunol.* **3**:609–620.
2. Sica, G., and Chen, L. 2000. Modulation of the immune response through 4-1BB. *Adv. Exp. Med. Biol.* **465**:355–362.
3. Vinay, D.S., and Kwon, B.S. 1998. Role of 4-1BB in immune responses. *Semin. Immunol.* **10**:481–489.
4. Watts, T.H. 2005. TNF/TNFR family members in costimulation of T cell responses. *Annu. Rev. Immunol.* **23**:23–68.
5. Guinn, B.A., et al. 2001. 4-1BBL enhances anti-tumor responses in the presence or absence of CD28 but CD28 is required for protective immunity against parental tumors. *Cell. Immunol.* **210**:56–65.
6. Martinet, O., et al. 2000. Immunomodulatory gene therapy with interleukin 12 and 4-1BB ligand: long- term remission of liver metastases in a mouse model. *J. Natl. Cancer Inst.* **92**:931–936.
7. Melero, I., et al. 1998. Amplification of tumor immunity by gene transfer of the co-stimulatory 4-1BB ligand: synergy with the CD28 co-stimulatory pathway. *Eur J. Immunol.* **28**:1116–1121.
8. Mogi, S., et al. 2000. Tumour rejection by gene transfer of 4-1BB ligand into a CD80 (+) murine squamous cell carcinoma and the requirements of co-stimulatory molecules on tumour and host cells. *Immunology.* **101**:541–547.
9. Ye, Z., et al. 2002. Gene therapy for cancer using single-chain Fv fragments specific for 4-1BB. *Nat. Med.* **8**:343–348.
10. Melero, I., et al. 1997. Monoclonal antibodies against the 4-1BB T-cell activation molecule eradicate established tumors. *Nat. Med.* **3**:682–685.
11. May, K.F., Jr., Chen, L., Zheng, P., and Liu, Y. 2002. Anti-4-1BB monoclonal antibody enhances rejection of large tumor burden by promoting survival but not clonal expansion of tumor-specific CD8+ T cells. *Cancer Res.* **62**:3459–3465.
12. Taraban, V.Y., et al. 2002. Expression and costimulatory effects of the TNF receptor superfamily members CD134 (OX40) and CD137 (4-1BB), and their role in the generation of anti-tumor immune responses. *Eur. J. Immunol.* **32**:3617–3627.
13. Miller, R.E., et al. 2002. 4-1BB-specific monoclonal antibody promotes the generation of tumor-specific immune responses by direct activation of CD8 T cells in a CD40-dependent manner. *J. Immunol.* **169**:1792–1800.
14. Wilcox, R.A., et al. 2002. Provision of antigen and CD137 signaling breaks immunological ignorance, promoting regression of poorly immunogenic tumors. *J. Clin. Invest.* **109**:651–659.
15. Hirano, F., et al. 2005. Blockade of B7-H1 and PD-1 by monoclonal antibodies potentiates cancer therapeutic immunity. *Cancer Res.* **65**:1089–1096.
16. Kocak, E., et al. 2006. Combination therapy with anti-CTL antigen-4 and anti-4-1BB antibodies enhances cancer immunity and reduces autoimmunity. *Cancer Res.* **66**:7276–7284.
17. Martinet, O., et al. 2002. T cell activation with systemic agonistic antibody versus local 4-1BB ligand gene delivery combined with interleukin-12 eradicate liver metastases of breast cancer. *Gene Ther.* **9**:786–792.
18. Ito, F., et al. 2004. Anti-CD137 monoclonal antibody administration augments the antitumor efficacy of dendritic cell-based vaccines. *Cancer Res.* **64**:8411–8419.
19. Waldmann, T.A., and Morris, J.C. 2006. Development of antibodies and chimeric molecules for cancer immunotherapy. *Adv. Immunol.* **90**:83–131.
20. Melero, I., Hervas-Stubbs, S., Glennie, M., Pardoll, D.M., and Chen, L. 2007. Immunostimulatory monoclonal antibodies for cancer therapy. *Nat. Rev. Cancer.* **7**:95–106.
21. Tuerk, C., and Gold, L. 1990. Systematic evolution of ligands by exponential enrichment: RNA ligands to bacteriophage T4 DNA polymerase. *Science.* **249**:505–510.
22. Ellington, A.D., and Szostak, J.W. 1990. In vitro selection of RNA molecules that bind specific ligands. *Nature.* **346**:818–822.
23. Gold, L. 1995. Oligonucleotides as research, diagnostic, and therapeutic agents. *J. Biol. Chem.* **270**:13581–13584.
24. White, R.R., Sullenger, B.A., and Rusconi, C.P. 2000. Developing aptamers into therapeutics. *J. Clin. Invest.* **106**:929–934.
25. Nimjee, S.M., Rusconi, C.P., and Sullenger, B.A. 2005. Aptamers: an emerging class of therapeutics. *Annu. Rev. Med.* **56**:555–583.
26. Ng, E.W., et al. 2006. Pegaptanib, a targeted anti-VEGF aptamer for ocular vascular disease. *Nat. Rev. Drug Discov.* **5**:123–132.
27. Dyke, C.K., et al. 2006. First-in-human experience of an antidote-controlled anticoagulant using RNA aptamer technology: a phase 1a pharmacodynamic evaluation of a drug-antidote pair for the controlled regulation of factor IXa activity. *Circulation.* **114**:2490–2497.
28. Santulli-Marotto, S., Nair, S.K., Rusconi, C., Sullenger, B., and Gilboa, E. 2003. Multivalent RNA aptamers that inhibit CTLA-4 and enhance tumor immunity. *Cancer Res.* **63**:7483–7489.
29. Harris, L.J., et al. 1992. The three-dimensional structure of an intact monoclonal antibody for canine lymphoma. *Nature.* **360**:369–372.
30. Alberts, B., et al. 2002. *Molecular biology of the cell.* 4th edition. Garland Science. New York, New York, USA/London, United Kingdom. 1616 pp.
31. Deane, J.A., and Bolland, S. 2006. Nucleic acid-sensing TLRs as modifiers of autoimmunity. *J. Immunol.* **177**:6573–6578.
32. Akira, S., Uematsu, S., and Takeuchi, O. 2006. Pathogen recognition and innate immunity. *Cell.* **124**:783–801.
33. Williams, B.R. 1999. PKR; a sentinel kinase for cellular stress. *Oncogene.* **18**:6112–6120.
34. Agrawal, S., and Kandimalla, E.R. 2004. Role of Toll-like receptors in antisense and siRNA [erratum 2005, **23**:117]. *Nat. Biotechnol.* **22**:1533–1537.
35. Marques, J.T., and Williams, B.R. 2005. Activation of the mammalian immune system by siRNAs. *Nat. Biotechnol.* **23**:1399–1405.
36. Haswell, L.E., Glennie, M.J., and Al-Shamkhani, A. 2001. Analysis of the oligomeric requirement for signaling by CD40 using soluble multimeric forms of its ligand, CD154. *Eur. J. Immunol.* **31**:3094–3100.
37. Holler, N., et al. 2003. Two adjacent trimeric Fas ligands are required for Fas signaling and formation of a death-inducing signaling complex. *Mol. Cell. Biol.* **23**:1428–1440.
38. Beigelman, L., et al. 1995. Chemical modification of hammerhead ribozymes. Catalytic activity and nuclease resistance. *J. Biol. Chem.* **270**:25702–25708.
39. Pieken, W.A., Olsen, D.B., Benseler, F., Aurup, H., and Eckstein, F. 1991. Kinetic characterization of ribonuclease-resistant 2'-modified hammerhead ribozymes. *Science.* **253**:314–317.
40. Tucker, C.E., et al. 1999. Detection and plasma pharmacokinetics of an anti-vascular endothelial growth factor oligonucleotide-aptamer (NX1838) in rhesus monkeys. *J. Chromatogr. B Biomed. Sci. Appl.*

732:203–212.
41. Willis, M.C., et al. 1998. Liposome-anchored vascular endothelial growth factor aptamers. *Bioconjug. Chem.* **9**:573–582.
42. Uno, T., et al. 2006. Eradication of established tumors in mice by a combination antibody-based therapy. *Nat. Med.* **12**:693–698.
43. Niu, L., et al. 2007. Cytokine-mediated disruption of lymphocyte trafficking, hemopoiesis, and induction of lymphopenia, anemia, and thrombocytopenia in anti-CD137-treated mice. *J. Immunol.* **178**:4194–4213.
44. Sun, Y., et al. 2002. Administration of agonistic anti-4-1BB monoclonal antibody leads to the amelioration of experimental autoimmune encephalomyelitis. *J. Immunol.* **168**:1457–1465.
45. Sun, Y., et al. 2002. Costimulatory molecule-targeted antibody therapy of a spontaneous autoimmune disease. *Nat. Med.* **8**:1405–1413.
46. Foell, J., et al. 2003. CD137 costimulatory T cell receptor engagement reverses acute disease in lupus-prone NZB x NZW F1 mice. *J. Clin. Invest.* **111**:1505–1518.
47. Seo, S.K., et al. 2004. 4-1BB-mediated immunotherapy of rheumatoid arthritis. *Nat. Med.* **10**:1088–1094.
48. Myers, L.M., and Vella, A.T. 2005. Interfacing T-cell effector and regulatory function through CD137 (4-1BB) co-stimulation. *Trends Immunol.* **26**:440–446.
49. Fitzwater, T., and Polisky, B. 1996. A SELEX primer. *Methods Enzymol.* **267**:275–301.
50. Sousa, R., and Padilla, R. 1995. A mutant T7 RNA polymerase as a DNA polymerase. *EMBO J.* **14**:4609–4621.
51. Wong, I., and Lohman, T.M. 1993. A double-filter method for nitrocellulose-filter binding: application to protein-nucleic acid interactions. *Proc. Natl. Acad. Sci. U. S. A.* **90**:5428–5432.
52. Layzer, J.M., and Sullenger, B.A. 2007. Simultaneous generation of aptamers to multiple gamma-carboxyglutamic acid proteins from a focused aptamer library using DeSELEX and convergent selection. *Oligonucleotides.* **17**:1–11.
53. Mathews, D.H., et al. 2004. Incorporating chemical modification constraints into a dynamic programming algorithm for prediction of RNA secondary structure. *Proc. Natl. Acad. Sci. U. S. A.* **101**:7287–7292.
54. Shuford, W.W., et al. 1997. 4-1BB costimulatory signals preferentially induce CD8+ T cell proliferation and lead to the amplification in vivo of cytotoxic T cell responses. *J. Exp. Med.* **186**:47–55.